

Electron-electron scattering in the intraband optical conductivity of Cu, Ag, and Au[†]

R. T. Beach and R. W. Christy

Department of Physics and Astronomy, Dartmouth College, Hanover, New Hampshire 03755

(Received 20 July 1977)

The predictions of the Drude dielectric function are compared with measured room-temperature reflectivities of the noble metals in the near infrared and visible regions. The electron scattering frequency $1/\tau$ is assumed to be the sum solely of electron-phonon scattering as calculated by Holstein and electron-electron scattering according to Gurzhi. The latter accounts for an important quadratic frequency dependence of $1/\tau$. Although Gurzhi's coefficient is too small by a factor of 2 to 4, an improved calculation by Lawrence gives more reasonable agreement with the data. In this comparison it is essential to consider the contribution to ϵ_1 from interband transitions at higher frequencies, which we derive from transmissivity measurements. The resulting reflectivity is in reasonable agreement with a selection of data for Cu and Au between 0.4 and 2.0 eV and for Ag between 0.4 and 3.3 eV, if the data are corrected for the anomalous skin effect, assuming some fraction of the electrons is diffusely scattered at the surface.

I. INTRODUCTION

The infrared optical properties of the noble metals are expected to be those of a free-electron Fermi gas, describable in terms of simple Drude theory. In this model the response of the gas to an electromagnetic wave is damped by $1/\tau$, the scattering frequency of the electrons. Experimental measurements of optical properties of the noble metals can usually be fit to the Drude formulas, but difficulties arise in the interpretation of $1/\tau$, especially with regard to its apparent wavelength dependence and its relation to the dc conductivity of the metal. The volume scattering mechanisms for free-conduction electrons include collisions with phonons, with other electrons, or with crystal imperfections—lattice defects and impurities. It is the purpose of this paper to show that selected room-temperature optical data for Cu, Ag, and Au can be satisfactorily fit to the one-carrier Drude formulas, assuming no other contributions to $1/\tau$ than from electron-phonon scattering and electron-electron scattering. We use the electron-phonon theory of Holstein¹ as applied by McKay and Rayne,² and the electron-electron theory of Gurzhi³ as improved by Lawrence.⁴ The only other experimental data needed are the dc conductivity, the Debye temperature, and the free-electron density.

The contribution to $1/\tau$ from each of these scattering mechanisms is independent of the others,³ so $1/\tau$ is just the sum

$$1/\tau = 1/\tau_\phi + 1/\tau_e + 1/\tau_i. \quad (1)$$

If the sample being studied is sufficiently pure and homogeneous, the contribution $1/\tau_i$ of imperfections will be negligible at room temperature. The Holstein theory of the infrared electron-phonon scattering $1/\tau_\phi$ has recently been confirmed ex-

perimentally for Cu, Ag, and Au by temperature-dependence studies² of the infrared absorptivity: $1/\tau_\phi$ increases significantly with T between 10 K and room temperature, and is independent of frequency throughout the middle infrared ($30 \mu\text{m} \geq \lambda \geq 3 \mu\text{m}$). In the near infrared and lower visible, however, up to the interband absorption edges, $1/\tau$ becomes strongly frequency dependent. The explanation of this dependence as due to electron-electron scattering $1/\tau_e$ has often been tentatively advanced for the noble metals⁵⁻⁸; a variety of optical experiments has yielded values for $1/\tau$ in the near infrared, but uncertainties in the results and discrepancies among various investigators, combined with the roughness of Gurzhi's theoretical expression for $1/\tau_e$, have made it impossible to do more than suggest the importance of $1/\tau_e$ in this region.

The purpose of what follows is to advance a model for $1/\tau$ in the near infrared, consisting of the sum of $1/\tau_\phi$ as given by Holstein and $1/\tau_e$ using the recent improvement by Lawrence in Gurzhi's order-of-magnitude expression for this scattering frequency. New measurements of reflectance and transmittance⁹ for Cu and Ag films in the near infrared and visible, coupled with some earlier measurements of reflectance^{6, 10-13} and transmittance¹⁴ on all three metals, will be used to test the model.

II. THEORY

A. Drude formula

The univalent noble metals have filled d bands plus one s electron in the conduction band, and a single-sheeted Fermi surface which is roughly equivalent to the free-electron Fermi sphere. Drude theory¹⁵ describes the intraband transitions of the conduction electrons. The complex dielec-

tric function $\hat{\epsilon} = \epsilon_1 + i\epsilon_2$ is given by

$$\epsilon_1 = 1 - \omega_p^2 / (\omega^2 + 1/\tau^2), \quad \epsilon_2 = \omega_p^2 / \omega (\omega^2 + 1/\tau^2) \tau,$$

where

$$\omega_p^2 = 4\pi N e^2 / m^*,$$

N being the density and m^* the band effective mass of the conduction electrons. The corresponding complex conductivity is related by $\hat{\epsilon} = 1 + i4\pi\hat{\sigma}/\omega$. For $\omega=0$ the dc conductivity is $\sigma(0) = \omega_p^2\tau/4\pi$. The damping of the electron gas in the Drude model is due to the same mechanisms for electron scattering as appear in the dc conductivity. One modification of these equations is essential for the noble metals. The onset of interband transitions sets an upper limit to the region where free-electron theory is sufficient, and the large interband absorption peaks have a significant effect on ϵ_1 at lower frequencies, in the free-electron intraband region. A term $\delta\epsilon_1$, associated with the absorption peaks at higher frequencies, must be added to ϵ_1 ; there is no correction to ϵ_2 . Also for the noble metals in the near infrared, $\omega\tau \gg 1$ always holds, so that we shall use

$$\epsilon_1 = 1 + \delta\epsilon_1 - \omega_p^2/\omega^2, \quad \epsilon_2 = \omega_p^2/\omega^2\tau. \quad (2)$$

Measurement of ϵ_1 over a wide spectral range yields ω_p and $\delta\epsilon_1$ from the slope¹⁶ and intercept of a plot of ϵ_1 vs $1/\omega^2$ (or λ^2); with ω_p known, data for ϵ_2 give $1/\tau$. The complex index of refraction $\hat{n} = n + ik = (\hat{\epsilon})^{1/2}$; thus

$$\epsilon_1 = n^2 - k^2, \quad \epsilon_2 = 2nk. \quad (3)$$

The Fresnel formulas¹⁷ express, in terms of n and k , the intensities R and T of, respectively, the reflected and transmitted fractions of a wave incident at an angle θ on a metallic slab of thickness d . The reflectivity R and the absorptivity A of a metal slab thick enough to be opaque ($T=0$) are simply related by $A = 1 - R$; at normal incidence ($\theta=0$)

$$A = 1 - R = 4n / [(n+1)^2 + k^2]. \quad (4)$$

For thinner films,

$$T = \frac{16n_3(n^2 + k^2) \exp(-2kd\omega/c)}{[(\hat{n}+1)(\hat{n}+n_3) - (\hat{n}-1)(\hat{n}-n_3) \exp(i2\hat{n}d\omega/c)]^2} \quad (5)$$

at normal incidence, where n_3 is the refractive index of the transparent substrate.

For Cu, Ag, and Au, $\hbar\omega_p \cong 9$ eV, so in the middle infrared (up to about 0.6 eV), $\omega \ll \omega_p$ and $(1 + \delta\epsilon_1)$ is negligible with respect to ω_p^2/ω^2 . In this region, $|\epsilon_1| \gg 1$; because $\omega\tau \gg 1$, $\epsilon_2 \ll |\epsilon_1|$ and $k \cong (-\epsilon_1)^{1/2}$. Since $k \gg n+1$, from Eq. (4)

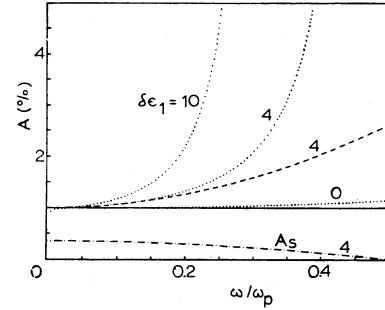


FIG. 1. Absorptivity as a function of frequency relative to the plasma frequency, assuming $\omega_p\tau=200$. Dotted curves: Drude absorptivity for various values of $\delta\epsilon_1$. Dashed curve: quadratic approximation to Drude absorptivity, Eq. (4b). Solid line: Mott-Zener formula, Eq. (4a). Dash-dotted curve: anomalous absorptivity, Eq. (10a), with $p=0$ for diffuse electron scattering.

$$A \cong 4n/k^2 \cong 2/\omega_p\tau. \quad (4a)$$

This expression for A in the infrared is the often-used^{1,2} Mott-Zener formula; it shows that the observed frequency independence of A (or R) in the middle infrared implies that $1/\tau$ is constant in this region. The next approximation for A does not neglect $(1 + \delta\epsilon_1)$ with respect to ω_p^2/ω^2 , nor 1 with respect to k^2 . The result is

$$A \cong (2/\omega_p\tau) [1 + \frac{1}{2}(3\delta\epsilon_1 + 1)(\omega^2/\omega_p^2)]. \quad (4b)$$

This expression demonstrates the importance of $\delta\epsilon_1$: Moving into the near infrared, A grows with frequency, the increase depending on $\delta\epsilon_1$, even if $1/\tau$ is constant. Figure 1 illustrates this effect. The dotted lines plot A vs ω/ω_p using Eqs. (2)–(4), for various values of $\delta\epsilon_1$, assuming constant $\omega_p\tau = 200$ —a typical value for noble metals. The dashed line is the approximate Eq. (4b) with $\delta\epsilon_1 = 4$, showing that this approximation to A is good up to $\omega/\omega_p \cong 0.2$ —somewhat less than 2 eV. The horizontal line is the Mott-Zener formula, Eq. (4a). The dash-dotted line will be discussed in Sec. II D.

B. Electron-phonon scattering

The scattering frequency $1/\tau$ in Eq. (2) includes the electron-phonon $1/\tau_\phi$, which is temperature dependent because the number of phonons depends strongly on the temperature T . In the infrared, Holstein's expression is^{1,2}

$$\frac{1}{\tau_\phi} = \frac{1}{\tau_0} \left[\frac{2}{5} + 4 \left(\frac{T}{\Theta} \right)^5 \int_0^{e/T} \frac{z^4 dz}{e^z - 1} \right], \quad (6)$$

where Θ is the Debye temperature and $1/\tau_0$ is a constant which must be independently determined. The derivation uses the simple Debye model for the phonon spectrum and is valid assuming E_F

$\gg \hbar\omega \gg k_B T, k_B \Theta$, where E_F is the electron Fermi energy. The coefficient $1/\tau_0$ may be evaluated from the known value of the dc conductivity, since for the dc case ($\hbar\omega \ll k_B T, k_B \Theta$) Holstein's expression is^{1,2}

$$\frac{1}{\tau_0(0)} = \frac{1}{\tau_0} \left[4 \left(\frac{T}{\Theta} \right)^5 \int_0^{\Theta/T} \frac{z^5 dz}{(e^z - 1)(1 - e^{-z})} \right]. \quad (7)$$

Knowing the dc conductivity $\sigma(0) = \omega_p^2 \tau / 4\pi$ yields $1/\tau_0$ if in the dc case $1/\tau$ is essentially $1/\tau_0(0)$ —a good assumption at room temperature where $1/\tau_i$ is certainly very small and where a temperature-dependent contribution to $1/\tau_e$ is negligible (see Sec. II C). A caveat is that the dc $1/\tau_0$ in Eq. (7) can differ from the infrared $1/\tau_0$ in Eq. (6) if $1/\tau_0$ is anisotropic on the Fermi surface,² although at room temperature isotropy would be expected.

C. Electron-electron scattering

Gurzhi's order-of-magnitude expression for $1/\tau_e$ is³

$$1/\tau_e \cong [\omega_p / (\hbar \omega_p)^2] [(k_B T)^2 + (\hbar\omega/2\pi)^2].$$

Using the Born approximation and Thomas-Fermi screening of the Coulomb interaction, Lawrence⁴ has made a more detailed calculation of the coefficient:

$$1/\tau_e = \frac{1}{12} \pi^3 \Gamma \Delta (1/\hbar E_F) [(k_B T)^2 + (\hbar\omega/2\pi)^2],$$

where Γ is a constant giving the average over the Fermi surface of the scattering probability, about 0.55 for the noble metals; Δ is the fractional umklapp scattering, about 0.75; E_F is the free-electron Fermi energy. This expression has been used⁴ to interpret low-temperature data on the dc electrical conductivity of the noble metals. Many-body effects enhance the Thomas-Fermi interaction in alkali metals,¹⁸ but not in the noble metals because of their relatively large d -band core polarizability.

The temperature-dependent term in $1/\tau_e$ is negligible in the infrared. Thus in the region of interest we use

$$1/\tau_e = \frac{1}{48} \pi \Gamma \Delta (1/\hbar E_F) (\hbar\omega)^2. \quad (8)$$

The coefficient of $(\hbar\omega)^2$ in Lawrence's expression for $1/\tau_e$ is larger than that in Gurzhi's by up to a factor of 2. Equation (8) begins to contribute significantly to $1/\tau$ only in the near infrared; in the middle infrared, $1/\tau \cong 1/\tau_0$.

Combining Eqs. (1), (4b), and (8), we get

$$A \cong (2/\omega_p \tau_0) \left[1 + \left(\frac{3}{2} \delta\epsilon_1 + \frac{1}{2} + 0.027 \hbar \omega_p^2 \tau_0 / E_F \right) \frac{\omega^2}{\omega_p^2} \right].$$

To this approximation, the ω^2 dependence of the electron-electron scattering is indistinguishable

from the contribution from $\delta\epsilon_1$, which could be as much as $\frac{1}{3}$ of the total ω^2 term. Therefore it is not possible to infer electron-electron scattering from a measurement of A (or R) alone, but it is essential to get $\delta\epsilon_1$ from an independent optical measurement—for example, T .

D. Surface scattering

In addition to the volume scattering mechanisms discussed above, collisions with the surface of the metal constitute another electronic decay mechanism which contributes to the absorption of photons. In the infrared, where the skin depth of the incident electromagnetic wave is comparable to the mean-free-path $v_F \tau$ of an electron (v_F is the electron Fermi velocity), it is not possible to assume that the electron current is proportional to the *local* electric field, as in the simple Drude model. The nonlocal deviation from Drude behavior,¹⁹ known as the anomalous skin effect, was calculated in detail by Dingle.²⁰ The result is presented as a total absorptivity A_t which includes both the Drude volume contribution and the "anomalous" surface absorption. The anomalous absorptivity depends upon how the electrons are reflected from the surface: for specular electron reflection it is negligible, but for diffuse scattering the total absorption A_t becomes

$$A_t = 4n_t / [(n_t + 1)^2 + k_t^2]$$

instead of Eq. (4), where, for thickness d much greater than the skin depth,

$$n_t + ik_t = \hat{n} - \frac{3}{16} \frac{v_F}{c} \left(\frac{\omega_p \tau}{1 - i\omega\tau} \right)^2 \left(\frac{\hat{n} - 1}{\hat{n} + 1} \right)^2.$$

The approximations which led to Eq. (4a) give

$$1 - R_t = A_t = A + A_s, \quad (9)$$

where the anomalous surface absorptivity

$$A_s \cong \frac{3}{4} v_F / c$$

amounts to a significant several tenths of a percent. Since $A_s \cong 0$ for specular scattering, this may be rewritten

$$A_s = \frac{3}{4} (v_F / c) (1 - p) \quad (10)$$

with p representing the fraction of electrons that are specularly scattered at the surface. The approximations used in Eq. (4b) give

$$A_s \cong \frac{3}{4} (v_F / c) (1 - p) [1 + (\delta\epsilon_1 - 8)(\omega^2 / \omega_p^2)], \quad (10a)$$

valid into the lower visible region. Equation (10a) is the dash-dotted curve in Fig. 1, with $\delta\epsilon_1 = 4$, $p = 0$, and $\frac{3}{4} v_F / c = 0.0035$ —all characteristic of the noble metals. The frequency dependence of A_s is clearly small compared with the large

changes in the standard Drude A , and so we use Eq. (10) hereafter. Dingle finds the correction to T to be negligible,

$$T_t = T. \quad (11)$$

III. DATA AND ANALYSIS

For Cu and Ag we are relying primarily on some new room-temperature measurements by Parkins⁹ of R and T for vacuum-evaporated films, over the spectral range 0.65 to 6.5 eV (1.9 to 0.19 μm). The experimental method is essentially that used by Johnson and Christy,¹⁴ with the major modification that the reflection measurements were made on opaque films using an absolute reflectance attachment. According to Dingle²⁰ the anomalous reflectance of a semitransparent film is dependent on the film thickness, and it will also depend on the refractive index of a supporting substrate. Reflectance measurements on opaque films avoid these difficulties in applying Dingle's theory. In addition Parkins's absolute R measurements on Cu avoid some uncertainty at the spectrophotometer detector change-point and are uniformly higher in the intraband region than the reflectivities of Ref. 14. Parkins's T measurements are in good agreement with Johnson and Christy's; the film thickness d is derived from the optical measurements. Other optical data used below include the reflectivities of Bennett and Ashley¹³ obtained on very carefully prepared thick evaporated films of Ag and Au. Hodgson⁶ measured the polarized internal reflectance of Au films in the near infrared. For Cu, handbook values due to Hass¹² for R of evaporated films were used. Bulk samples are represented by McKay and Rayne's absorptivities² measured calorimetrically, and by the ellipsometric results of Roberts¹⁰ on

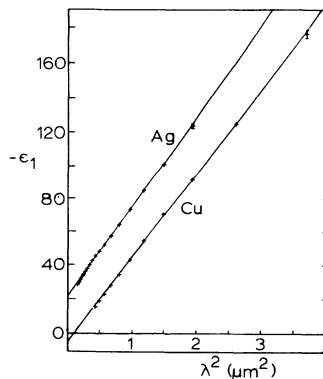


FIG. 2. Negative of the real dielectric constant vs wavelength squared, from Parkins's data (Ref. 9). The curve for Ag is displaced upwards by 25 for clarity.

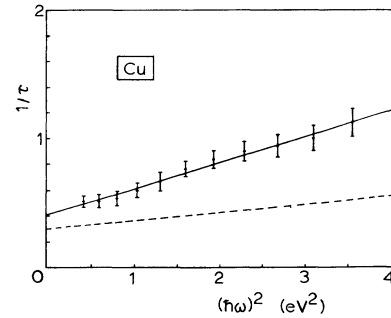


FIG. 3. Electron scattering frequency in units of 10^{14} sec^{-1} for Cu vs photon energy squared. Solid line: least-squares fit to Parkins's data (Ref. 9). Dashed line: calculated from theory, Eqs. (6) and (8).

Cu and Otter¹¹ on Ag. For Au we used Johnson and Christy's T values.¹⁴

Our procedure in comparing the optical measurements with the theory was first to use Parkins's complete data on Cu and Ag in order to derive values for the optical parameters appearing in Eqs. (1)–(11), by fitting the data to the functional form of the equations. [We did *not* use the approximations of Eqs. (4a) or (4b).] Diffuse scattering ($p=0$) is assumed, as it seems to be the rule in all but the most ideal samples. With $p=0$ in Eq. (10), A_s was added to Parkins's experimental R_t to give the Drude R ; following Dingle, no correction to T was required. The R 's and T 's were then inverted according to Eqs. (4) and (5) to obtain values for n and k corrected for the anomalous skin effect, and therefore representative purely of the volume optical properties of the metal. The corrected k 's differed little from their uncorrected values; the corrected n 's were significantly lower, showing the sensitivity of n —and the insensitivity of k —to the value of R .

From Eqs. (3), n and k gave ϵ_1 and ϵ_2 ; then

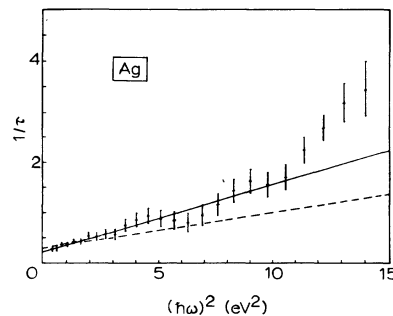


FIG. 4. Electron scattering frequency in units of 10^{14} sec^{-1} for Ag vs photon energy squared. Solid line: least-squares fit to Parkins's data (Ref. 9). Dashed line: calculated from theory, Eqs. (6) and (8).

TABLE I. Numerical values of the fixed parameters used in the model.

	Cu	Ag	Au	Ref.
N (10^{22} cm $^{-3}$)	8.52	5.90	5.93	2
v_F (10^8 cm/sec)	1.57	1.39	1.39	21
E_F (eV)	7.00	5.48	5.51	21
Γ	0.57	0.55	0.55	4
Δ	0.79	0.73	0.77	4
Θ (K)	310	220	185	22
$1/\sigma(0)$ ($\mu\Omega$ cm)	1.80	1.16	1.32	22

plots of $-\epsilon_1$ vs λ^2 yielded ω_p and $\delta\epsilon_1$. (See Fig. 2.) The least-squares method was used for all lines fit to data. From Eq. (2), ϵ_2 and ω_p give $1/\tau = \omega^3\epsilon_2/\omega_p^2$. Equation (8) predicts that $1/\tau_e \propto (\hbar\omega)^2$, so the appropriate plot is $1/\tau$ vs photon energy squared. (See Figs. 3 and 4.) The $\omega=0$ intercept of these plots should yield the electron-phonon scattering frequency $1/\tau_\phi$. Knowing $1/\tau_\phi$ gives the infrared $1/\tau_0$ via Eq. (6) for comparison with the dc $1/\tau_0$ determined independently from the dc conductivity $\sigma(0)$ and Eq. (7).

As a second procedure, which permits comparison of the theory with other experimental reflectance data, for all three metals, we calculated R from Eqs. (1)–(10), using as input the values of the parameters derived in the first procedure.

Free-electron values²¹ for v_F and E_F are employed in Eqs. (8) and (10). White and Woods's values²² for $\sigma(0)$ at $T=\Theta$ are used; following them, the Debye temperature Θ is assumed to be the high-temperature specific-heat value. Table I summarizes the fixed parameters used in the model.

IV. RESULTS AND DISCUSSION

Figure 2 presents the values of ϵ_1 for Cu and Ag from which m^* and $\delta\epsilon_1$ are derived. Since in the near infrared $-\epsilon_1 = k^2$ and k is determined almost solely by the transmission measurement, the accuracy of the ϵ_1 data reflects the error in

the measurement of the transmissivity T . The error in k was estimated from the spread in values of k calculated using the same reflectances but different T 's obtained from transmission measurements on films of different thicknesses. This technique also gave the error in n due to the uncertainty in T . Parkins's reflectance measurements have an estimated error of ± 0.0005 . Although there is a significant contribution to the error in n from both the uncertainties in R and T , n is most sensitive to R . Figures 3 and 4 show the derived values of $1/\tau$. The size of the error bars is mainly due to the percentage error in n , since n is very small over the range of interest.

In fitting Parkins's Cu and Ag data, at first the same spectral range, 0.6 to 2.0 eV, was used for both metals. In Cu, interband transitions begin at about 2 eV; in Ag, at about 4 eV. Thus, for the latter there is an additional 2-eV range where Drude theory is expected to hold. We found that in Ag the original linear fits of $-\epsilon_1$ to λ^2 and $1/\tau$ to $(\hbar\omega)^2$ could be extended—with only very slight changes in the resulting slopes and intercepts—to include photon energies up to 3.3 eV. Above 3.3 eV, $1/\tau$ rises more sharply; this behavior could be due to a tail of the absorption edge.²³ Thus in Figs. 2 and 4 we use the least-squares fits to the Ag data over the range 0.6 to 3.3 eV, but the four points above 3.3 eV in Fig. 4 are not used in the fit. The solid lines in Figs. 2–4 show the least-squares fits. The slopes and intercepts in Fig. 2 for Cu and Ag are listed in Table II, along with some values from the literature.

The dashed lines in Figs. 3 and 4 show $1/\tau$ as predicted by the theoretical model. The theoretical $1/\tau_\phi$ is calculated from $1/\tau_0$ given by the dc conductivity, assuming that at 293 K electron-phonon scattering is isotropic and that $1/\tau = 1/\tau_\phi$ at $\omega=0$. The frequency dependence is given by Lawrence's $1/\tau_e$ in Eq. (8). For the slope $\beta = d(1/\tau)/d(\hbar\omega)^2$ of the dashed lines, the approximations used to derive the theoretical $1/\tau_e$ make agreement with experiment to within a factor of 2 reasonable. What is most important is that

TABLE II. Values for the optical effective mass m^* and $\delta\epsilon_1$ from Fig. 2 (Parkins) and from the literature.

	Cu		Ag		Au	
	m^*/m	$\delta\epsilon_1$	m^*/m	$\delta\epsilon_1$	m^*/m	$\delta\epsilon_1$
Parkins (Ref. 9)	1.54	4.1	0.99	2.4
Johnson (Ref. 14)	1.49	6	0.96	2	0.99	9
Ehrenreich (Ref. 24)	1.42	4.7	1.03	2.3	1.04	...
Thèye (Ref. 7)	0.87	...	0.94	6
Hodgson (Ref. 6)	0.96	6

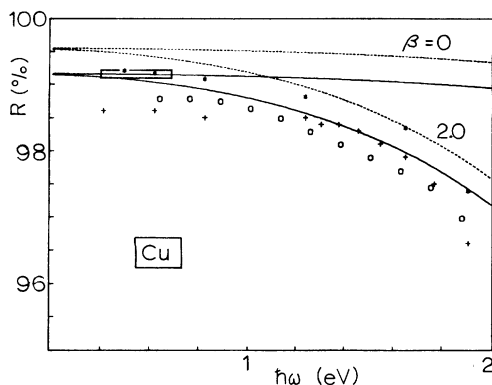


FIG. 5. Reflectivity as a function of photon energy for Cu at room temperature. Solid curves are calculated assuming $p=0$ for diffuse scattering, dashed assuming $p=1$ for specular scattering (Drude reflectivity), with electron-phonon scattering frequency from dc conductivity. With $\beta=0$, electron-electron scattering is neglected; it is included with $\beta=2.0 \times 10^{13} \text{ sec}^{-1} \text{ eV}^{-2}$. Reflectance: \circ Parkins (Ref. 9), $+$ Hass (Ref. 12); $*$ Roberts (Ref. 10), ellipsometric; \square McKay and Rayne (Ref. 2), calorimetric.

$1/\tau$ varies as ω^2 ; for both Cu and Ag a quadratic frequency dependence fits Parkins's data better than a linear or cubic one. The values of the slopes and intercepts of the experimental and calculated lines in Figs. 3 and 4 are listed in Table III. For Ag the numerical values for β and $1/\tau_\phi$ are in agreement within error; for Cu the values for β and $1/\tau_\phi$ are not so close, but still perhaps within the expected error. It may be noted (Table II) that the value of m^*/m derived from Parkins's Cu data is on the high end of the range; using $m^*/m=1.42$ instead would yield experimental entries for $\beta(1.86)$ and $1/\tau_\phi(3.78)$ which are closer to the model.

As a second mode of comparing the theory with data, we noted that the model for $1/\tau$ could be used to calculate reflectivities if values of ω_p and $\delta\epsilon_1$ are chosen. Such curves are plotted in Figs. 5-7, along with reflectivity data from Parkins and from the literature. The solid theoretical curves represent $p=0$; the dashed, $p=1$. For Cu and Ag, ω_p and $\delta\epsilon_1$ were taken from Parkins's results; for Au, the values obtained by Johnson and Christy were used. For $1/\tau_\phi$ we used in each case the

TABLE III. Values for the slope $\beta=d(1/\tau)/d(\hbar\omega)^2$ and the intercept $1/\tau_\phi$ of the experimental and calculated curves in Figs. 3 and 4.

	Cu		Ag	
	Expt	Calc	Expt	Calc
$\beta (10^{13} \text{ sec}^{-1} \text{ eV}^{-2})$	2.01	0.63	1.34	0.73
$1/\tau_\phi (10^{13} \text{ sec}^{-1})$	4.09	2.98	2.15	2.80

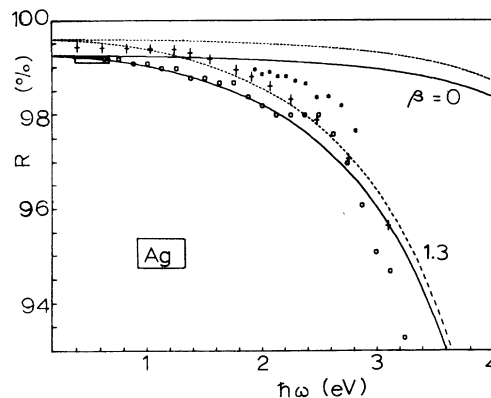


FIG. 6. Reflectivity as a function of photon energy for Ag at room temperature. Solid curves are calculated assuming $p=0$ for diffuse scattering, dashed assuming $p=1$ for specular scattering (Drude reflectivity), with electron-phonon scattering frequency from dc conductivity. With $\beta=0$, electron-electron scattering is neglected; it is included with $\beta=1.3 \times 10^{13} \text{ sec}^{-1} \text{ eV}^{-2}$. Reflectance: \circ Parkins (Ref. 9), $+$ Bennett and Ashley (Ref. 13); $*$ Otter (Ref. 11), ellipsometric; \square McKay and Rayne (Ref. 2), calorimetric.

values calculated from the dc conductivity according to Holstein's formulas. For β , the slope of $1/\tau_\phi$, the experimental values derived above were used for Cu and Ag (2.01 and $1.34 \times 10^{13} \text{ sec}^{-1} \text{ eV}^{-2}$, respectively), and an estimated value was used for Au (0.99). The agreement with the experimental data is generally good, although for each metal the experimental points fall faster than the theoretical curves at energies just below the onset

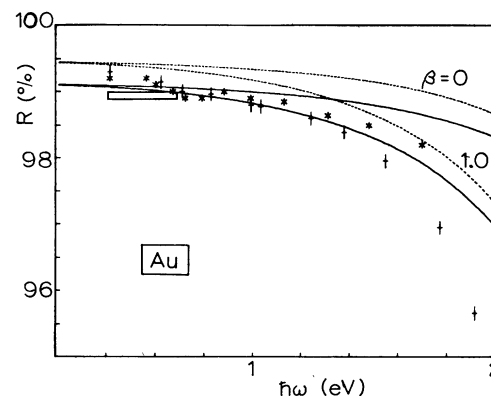


FIG. 7. Reflectivity as a function of photon energy for Au at room temperature. Solid curves are calculated assuming $p=0$ for diffuse scattering, dashed assuming $p=1$ for specular scattering (Drude reflectivity), with electron-phonon scattering frequency from dc conductivity. With $\beta=0$, electron-electron scattering is neglected; it is included with $\beta=1.0 \times 10^{13} \text{ sec}^{-1} \text{ eV}^{-2}$. Reflectance: $+$ Bennett and Ashley (Ref. 13); $*$ Hodgson (Ref. 6), polarimetric; \square McKay and Rayne (Ref. 2), calorimetric.

of interband transitions. This behavior is due to the increase of $\delta\epsilon_1$ near the absorption edge,²⁴ the effect of which can also be seen in Fig. 2. The bulk-sample values we selected happen to lie higher than the film values, though not by more than their experimental error. We are uncertain how to treat the anomalous skin effect in the reflectivities computed from the ellipsometric results.^{10, 11} Also included for comparison are reflectivity curves calculated assuming no electron-electron interaction—that is, $\beta=0$ (but the same values for all the other parameters). It is clear that the assumed electron-electron contribution is important in all three metals.

V. CONCLUSIONS

The model presented above assumes that the volume optical properties of the noble metals in the near infrared and red may be understood according to the Drude theory, with electron scattering by just two basic interactions: electron-phonon and electron-electron. The latter of these contributes a significant wavelength dependence to the electron scattering frequency $1/\tau$. Considering the experimental difficulties in measuring $1/\tau$, and the uncertainties in the theory behind the electron scattering rate, we regard the agreement of model with data as good. It is satisfactory for Ag, which of the noble metals has the largest region in which its behavior is Drudelike; it is poorer for Cu, which presents the most severe experimental problems. Nevertheless, the discrepancy for Cu suggests that it might be worthwhile to incorporate band effects into the electron-electron calculation, since only for Cu does the band effective mass differ appreciably from 1.

The quadratic frequency dependence of $1/\tau$ is an important test of electron-electron scattering.²⁵ The frequency dependence of Holstein's electron-phonon formula is negligible far above $k_B\Theta/\hbar$ (≈ 0.03 eV). In his calculation it is assumed that $\hbar\omega \ll E_F$, but a free-electron density-of-states average would contribute a negative correction to $1/\tau_\phi$ of $\frac{1}{2}(\hbar\omega/E_F)^2$; this is negligible even at $\hbar\omega \approx \frac{1}{2}E_F$ in comparison to the electron-electron term. Other mechanisms for a ω^2 dependence are possible—in particular, a two-carrier model. This seems inapplicable here, although it might be applicable in the transition-metal case, where much larger values of $\beta = d(1/\tau)/d(\hbar\omega)^2$ have been inferred.^{16, 26} (An effective-mass modification in the electron-electron term would also be larger for narrow d bands.) A two-carrier model²⁷ might also make an additional contribution in those cases of noble-metal films for which a structure dependence of β is observed.^{7, 28} In summary we believe that the electron-electron scattering mechanism provides the best explanation of the data discussed above. A similar conclusion about its importance for Al in the middle infrared has been reported.²⁹ The predicted temperature independence of β for electron-electron scattering has yet to be convincingly tested.

We conclude that optical measurements on the noble metals may furnish a useful test of electron-electron scattering calculations.

ACKNOWLEDGMENTS

We are very grateful to Professor W. E. Lawrence for many helpful discussions and to G. R. Parkins for permission to use his unpublished data.

†Work supported by the NSF.

¹T. Holstein, *Ann. Phys. (N.Y.)* **29**, 410 (1964); *Phys. Rev.* **96**, 535 (1954).

²J. A. McKay and J. A. Rayne, *Phys. Rev. B* **13**, 673 (1976).

³R. N. Gurzhi, *Zh. Eksp. Teor. Fiz.* **33**, 660 (1957) [*Sov. Phys.-JETP* **6**, 506 (1958)]; **35**, 965 (1958) [*Sov. Phys.-JETP* **8**, 673 (1959)]. R. N. Gurzhi, M. Y. Azbel', and H. P. Lin, *Fiz. Tverd. Tela.* **5**, 759 (1963) [*Sov. Phys.-Solid State* **5**, 554 (1963)].

⁴W. E. Lawrence, *Phys. Rev. B* **13**, 5316 (1976), and (private communication).

⁵H. E. Bennett and J. M. Bennett, *Proceedings of the International Colloquium on Optical Properties, Paris, 1965*, edited by F. Abelès (North-Holland, Amsterdam, 1966), p. 175. H. E. Bennett, J. M. Bennett, E. J. Ashley, and R. J. Motyka, *Phys. Rev.* **165**, 755 (1968).

⁶J. N. Hodgson, *J. Phys. Chem. Solids* **29**, 2175 (1968).

⁷M. L. Thèye, *Phys. Rev. B* **2**, 3060 (1970); M. M. Du-jardin and M. L. Thèye, *J. Phys. Chem. Solids* **32**,

2033 (1971).

⁸P. B. Johnson and R. W. Christy, *Phys. Rev. B* **11**, 1315 (1975).

⁹G. R. Parkins and R. W. Christy (unpublished).

¹⁰S. Roberts, *Phys. Rev.* **118**, 1509 (1960).

¹¹M. Otter, *Z. Phys.* **161**, 163 (1961).

¹²G. Hass, *American Institute of Physics Handbook*, edited by D. E. Gray (McGraw-Hill, New York, 1963), 2nd ed., p. 6-108.

¹³J. M. Bennett and E. J. Ashley, *Appl. Opt.* **4**, 221 (1965).

¹⁴P. B. Johnson and R. W. Christy, *Phys. Rev. B* **6**, 4370 (1972).

¹⁵See, for example, R. W. Christy, *Am. J. Phys.* **40**, 1403 (1972).

¹⁶J. W. Allen and J. C. Mikkelsen, *Phys. Rev. B* **15**, 2952 (1977). In general ω_p depends on ω if τ does, but we will find that ω_p is practically constant within our range.

¹⁷See, for example, J. E. Nestell and R. W. Christy,

- Am. J. Phys. 39, 313 (1971).
- ¹⁸C. A. Kukkonen, Ph.D. thesis (Cornell University, 1975) (unpublished).
- ¹⁹T. Holstein, Phys. Rev. 88, 1427 (1952).
- ²⁰R. B. Dingle, Physica (Utr.) 19, 311, 348, 729, 1187 (1953).
- ²¹C. Kittel, *Introduction to Solid State Physics*, 4th ed. (Wiley, New York, 1971), p. 248.
- ²²G. K. White and S. B. Woods, Philos. Trans. R. Soc. Lond. A 251, 273 (1958).
- ²³M. Guerrisi, R. Rosei, and P. Winsemius, Phys. Rev. B 12, 557, 4570 (1975).
- ²⁴H. Ehrenreich and H. R. Philipp, Phys. Rev. 128, 1622 (1962); B. R. Cooper, H. Ehrenreich, and H. R. Philipp, Phys. Rev. 138, A494 (1965).
- ²⁵We note that a quadratic dependence is expected as a first approximation in any analytic scattering theory. See Ref. 16.
- ²⁶J. J. Hopfield, AIP Conf. Proc. 4, 358 (1972).
- ²⁷S. R. Nagel and S. R. Schnatterly, Phys. Rev. B 9, 1299 (1974).
- ²⁸J. Rivory, Phys. Rev. B 15, 3119 (1977).
- ²⁹T. J. Wieting and J. T. Schriempf, Bull. Am. Phys. Soc. 20, 334 (1975).